



Alternating current magnetotransport in $\text{Sm}_{0.1}\text{La}_{0.6}\text{Sr}_{0.3}\text{MnO}_3$

M. Aparnadevi and R. Mahendiran

Citation: *AIP Advances* **3**, 012114 (2013); doi: 10.1063/1.4789408

View online: <http://dx.doi.org/10.1063/1.4789408>

View Table of Contents: <http://scitation.aip.org/content/aip/journal/adva/3/1?ver=pdfcov>

Published by the AIP Publishing

Articles you may be interested in

[Electrical detection of spin reorientation transition in ferromagnetic \$\text{La}_{0.4}\text{Sm}_{0.3}\text{Sr}_{0.3}\text{MnO}_3\$](#)

J. Appl. Phys. **113**, 17D719 (2013); 10.1063/1.4797471

[Impact of Fe doping on radiofrequency magnetotransport in \$\text{La}_{0.7}\text{Sr}_{0.3}\text{Mn}_{1-x}\text{Fe}_x\text{O}_3\$](#)

J. Appl. Phys. **111**, 07D728 (2012); 10.1063/1.3680218

[Magnetic proximity effect in \$\text{Pr}_{0.5}\text{Ca}_{0.5}\text{MnO}_3/\text{La}_{0.7}\text{Sr}_{0.3}\text{MnO}_3\$ bilayered films](#)

Low Temp. Phys. **38**, 41 (2012); 10.1063/1.3677235

[Dynamical magnetotransport in \$\text{Ln}_{0.6}\text{Sr}_{0.4}\text{MnO}_3\$ \(Ln=La, Sm\)](#)

J. Appl. Phys. **109**, 07C728 (2011); 10.1063/1.3562517

[Softening of the first-order magnetic phase transition and magnetotransport properties of \$\text{Sm}_{0.55}\text{Sr}_{0.45}\text{MnO}_3\$ manganite](#)

J. Appl. Phys. **104**, 093915 (2008); 10.1063/1.3010308

NEW Special Topic Sections

NOW ONLINE
Lithium Niobate Properties and Applications:
Reviews of Emerging Trends

AIP Applied Physics Reviews

Alternating current magnetotransport in $\text{Sm}_{0.1}\text{La}_{0.6}\text{Sr}_{0.3}\text{MnO}_3$

M. Aparnadevi and R. Mahendiran^a

Department of Physics, 2 Science Drive 3, Faculty of Science, National University of Singapore, Singapore 117542, Singapore

(Received 19 November 2012; accepted 10 January 2013; published online 16 January 2013)

We report frequency dependent ($f = 0.1$ to 5 MHz) electrical resistivity in $\text{Sm}_{0.1}\text{La}_{0.6}\text{Sr}_{0.3}\text{MnO}_3$ in superimposed dc magnetic fields ($H = 0$ –1 kOe). Resistive (ρ') and reactive (ρ'') components of the complex resistivity ($\rho = \rho' + i\rho''$) were measured simultaneously. With increasing f , both ρ' and ρ'' increase abruptly at the onset of ferromagnetic transition ($T_c = 348$ K) and exhibit an anomaly at $T^* \approx 147$ K $\ll T_c$ in $H = 0$ kOe. The observed features in ρ' and ρ'' are depressed with increasing H leading to 35% magnetoresistance for $\Delta H = 300$ Oe and $f = 3$ MHz. It is suggested that the frequency dependent magnetotransport is dominated by the field and frequency dependences of the ac permeability. Copyright 2013 Author(s). This article is distributed under a Creative Commons Attribution 3.0 Unported License. [<http://dx.doi.org/10.1063/1.4789408>]

I. INTRODUCTION

Since the discovery of colossal magnetoresistance in perovskite manganites (example $\text{La}_{0.7}\text{Sr}_{0.3}\text{MnO}_3$) nearly two decades ago, numerous investigations have focused on electrical resistivity and magnetoresistance measured with direct current (dc).¹ Dc electrical conduction in these materials is due to spin polarized hopping of e_g holes between Mn^{4+} and Mn^{3+} ions in the background of immobile t_{2g}^3 spins along the $\text{Mn}^{4+}(t_{2g}^3e_g^0)\text{-O}^{2-}\text{-Mn}^{4+}(t_{2g}^3e_g^1)$ network. According to the well accepted Zener's double exchange mechanism, ferromagnetic alignment of t_{2g} spins leads to lower resistivity (ρ) and metallic type conduction ($d\rho/dT > 0$) and antiferromagnetic alignment leads to increase in resistivity.² In the spin disordered paramagnetic state, dynamical/static Jahn-Teller distortion causes self localization of charge carriers in the form of polarons which leads to insulating behavior of resistivity ($d\rho/dT < 0$).

An interesting question is what happens to the electrical resistivity and magnetoresistance if the charge carriers (e_g holes) are subjected to an alternating (ac) current. Surprisingly, very little work have been done so far on the dynamical electrical and magnetotransport in manganites. Electrical response of insulating manganites (RMnO_3 where $R = \text{Tb, Gd, Dy, and also Bi}$) to alternating electrical field in kHz frequency range ($f = 1$ –10 kHz) in presence of magnetic field is a topic of current interest due to coupling between magnetic and electrical dipoles that leads to magnetically tunable capacitance or electrical polarization in some manganites.^{3,4} Few researchers focused their attention on intrinsic or extrinsic contributions to the magnetocapacitance utilizing impedance spectroscopy measured over a wider frequency range ($f \sim 100$ Hz–1 MHz) in so-called multiferroics.^{5,6} On the other hand, Bhagat *et al.*⁷ investigated microwave ($f = 10$ GHz) surface impedance in metallic $\text{La}_{0.67}\text{Ba}_{0.33}\text{MnO}_3$ and found that it varied dramatically in small dc magnetic fields (= 38% in $H = 300$ Oe at $f = 10$ GHz). Schwartz *et al.*⁸ extracted spontaneous magnetization of the ferromagnetic metallic $\text{La}_{0.8}\text{Sr}_{0.2}\text{MnO}_3$ single crystal from studies of zero-field surface impedance ($f = 0.045$ –45 GHz) as a function of temperature and frequency. In the above experiments, the samples were subjected to a microwave magnetic field and the surface impedance

^a Author for correspondence (E-mail: phyrm@nus.edu.sg)



was calculated from the power absorbed by sample in microwave cavity. However, four-probe ac electrical response of ferromagnetic metallic manganites in the lower end of radio frequency spectrum ($f = 1$ kHz to 20 MHz) has been seldom reported. A few available reports^{9,10} suggest that the magnitude of the magnetoresistance in sub-kilogauss magnetic fields is greatly enhanced with ac current excitation, but the mechanism of ac magnetoresistance as well as factors affecting the ac magnetoresistance are not clearly understood yet.

The purpose of this letter is to investigate radiofrequency (*rf*) electrical transport in a La substituted $\text{Sm}_{0.7-x}\text{La}_x\text{Sr}_{0.3}\text{MnO}_3$ sample both as a function of temperature and magnetic field. We were partly motivated by our earlier observation of unusual double magnetic phase transitions in $\text{Sm}_{0.6-x}\text{La}_x\text{Sr}_{0.4}\text{MnO}_3$ series.¹¹ The field-cooled magnetization of compounds in this series, with the exception of the end member ($x = 0.6$), showed anomalous decrease of magnetization below a temperature T^* within the long-range ferromagnetic state. We suggested that the anomalous decrease of magnetization is due to ordering of Sm-4f moments antiparallel to the Mn-sublattice and possible spin reorientation transition. The ordering of Sm-4f is driven by the molecular field of Mn sublattice. Ordering of Sm moment in the parent antiferromagnetic SmMnO_3 causes negative magnetization below the compensation point $T_{\text{comp}} = 9.4$ K.^{12,13} Ac magnetotransport in these compounds has not been reported so far.

II. EXPERIMENT DETAILS

Polycrystalline $\text{Sm}_{0.7-x}\text{La}_x\text{Sr}_{0.3}\text{MnO}_3$ ($x = 0, 0.2, 0.4, 0.6$, and 0.7) samples were prepared by the standard solid state reaction method. Powder X-ray diffraction revealed that the samples are single phase. Four probe ac impedance ($Z = R + iX$) of the samples was measured using an Agilent 4294A impedance analyzer that was interfaced to a Physical Property Measuring System (PPMS), which provided a platform for varying temperature and magnetic field. Both in-phase (ρ') and out of phase (ρ'') components of the complex resistivity ($\rho = \rho' + i\rho''$) as a function of frequency ($f = 0.1$ – 5 MHz) were calculated from simultaneous measurements of ac resistance (R) and reactance (X), respectively. The distance between the voltage probes was fixed to 2.7 mm and current pads were attached to the ends of 6.8 mm long rectangular sample. The ac current through the sample was 5 mA (*rms*) and the measured values of R and X were found to be independent of current amplitudes from 1 mA up to 20 mA. The dc magnetic field was applied parallel to the direction of ac current in the sample. The dc magnetization and dc resistivity were also measured with a vibrating sample magnetometer and the PPMS.

III. RESULTS

Fig. 1(a) compares temperature dependences of the dc magnetization (M) of $\text{Sm}_{0.7-x}\text{La}_x\text{Sr}_{0.3}\text{MnO}_3$ ($x = 0.0, 0.2, 0.4, 0.6$ and 0.7) measured while cooling under $H = 1$ kOe from 400 K to 10 K. The steep increase of $M(T)$ at $T_c = 372$ K for $x = 0.7$ indicates paramagnetic (PM) to ferromagnetic (FM) transition upon cooling. While the T_c decreases to 348 K for $x = 0.6$, $M(T)$ shows a broad maximum around $T^* = 147$ K below which it decreases continuously with decreasing temperature. As the Sm content increases, both T_c and T^* decrease ($T_c = 348, 256, 123$ and 83 K, $T^* = 147, 59, 56, 30$ K for $x = 0.6, 0.4, 0.2$ and 0 , respectively). In order to check whether the observed behavior is due to cluster or spin glass transition, we measured $M(T)$ under different dc magnetic fields for $x = 0.6$, which are shown in Fig. 1(b). The zero field cooled (ZFC) and field cooled (FC) magnetization curves diverge below 150 K for $H = 100$ Oe and 300 Oe. However, differences between the FC and ZFC magnetizations become negligible for fields at and above $H = 500$ Oe. The T^* is close to 150 K for $H = 100$ Oe and it gradually shifts down with increasing strength of H . The field-cooled $M(T)$ is expected to slowly increase below the spin or cluster freezing temperature unlike the decrease found in our compounds, which rules out the possibility that the low temperature anomaly is due to cluster glass like transition. The inset of Fig. 1(c) compares M - H isotherms at three temperatures ($T = 10, 150$ and 250 K). We show the data only up to 15 kOe though we have measured up to 50 kOe. The M - H curves show typical ferromagnetic behavior below T_c but the value of M for $H < 10$ kOe progressively decreases as T lowers below T^* , which is in agreement with the

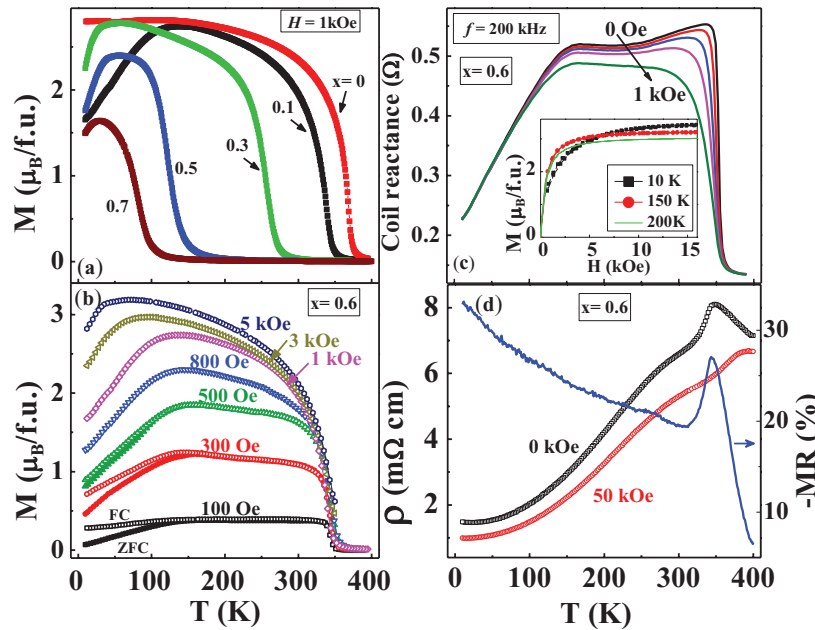


FIG. 1. Temperature dependence of (a) field-cooled magnetization (M) in $\text{Sm}_{0.7-x}\text{La}_x\text{Sr}_{0.3}\text{MnO}_3$ ($x = 0, 0.2, 0.4, 0.6$ and 0.7) for $H = 1 \text{ kOe}$, (b) M under different dc magnetic fields (H) for $x = 0.6$ sample in zero field cooled (ZFC, open symbols) and field-cooled modes (FC, closed symbols), (c) Inductive reactance (X) of 10-turn copper coil wound on the sample under different dc magnetic fields H . Inset compares $M(H)$ isotherms at $T = 10, 150$ and 200 K . (d) Dc resistivity for $H = 0$ and 50 kOe . The magnetoresistance (MR) is also shown on the right scale.

behavior of dc $M(T)$ data below T^* . For $H > 10 \text{ kOe}$, $M(H)$ tends to increase with lowering temperature as expected for a normal ferromagnet. The main panel of Fig. 1(c) shows the ac reactance X ($f = 200 \text{ Hz}$) of a 10-turn copper coil tightly wound around the middle of a 10 mm-long sample under different dc magnetic fields applied parallel to the length of the sample. The reactance of the coil is proportional to the in-phase component of the ac permeability (μ') of the sample. The sharp increase in $X(T)$ around 348 K in the absence of an external magnetic field indicates the onset of ferromagnetic ordering and the rapid decrease below $T^* = 147 \text{ K}$ is in agreement with the low field dc $M(T)$. The applied dc magnetic field reduces the value of X in the temperature region between T_c and T^* , but not above T_c or below T^* . Fig. 1(d) shows the dc resistivity (ρ) of the sample under $H = 0$ and 50 kOe . The $\rho(H = 0 \text{ Oe})$ shows an insulator-metal transition with a peak at T_c . The resistivity decreases in magnitude and the peak shifts above 400 K under $H = 50 \text{ kOe}$ leading to a negative magnetoresistance of 27% at T_c and 33% at the lowest temperature. The metallic behavior of the sample below T_c in zero field also rules out the spin or cluster glass transition in the Mn sublattice.

Four probe rf electrical transport in the sample was measured at several frequencies of the ac current ($f = 0.1$ to 5 MHz). We show the data for only selected frequencies for clarity. Left panel of Figure 2 shows the in-phase component, i.e., ac resistivity, $\rho'(T)$ under superimposed dc magnetic fields ($H = 0, 300, 500, 700 \text{ Oe}$ and 1 kOe) for (a) $f = 200 \text{ kHz}$, (b) 1 MHz and (c) 5 MHz . The behavior of $\rho'(T)$ at 200 kHz is similar to the dc $\rho(T)$ and its magnitude is hardly affected in low magnetic fields. By contrast, $\rho'(T)$ for $f = 1 \text{ MHz}$ in $H = 0 \text{ Oe}$ shows a steep increase at $T = 348 \text{ K}$ and a peak nearby. Then, it decreases gradually until 170 K and shows a kink around $T^* \sim 147 \text{ K}$, which closely resembles the low-field dc magnetization data. The peak at T_c decreases in magnitude and shifts to lower temperature with increasing H and completely disappears for $H = 1 \text{ kOe}$. The kink at T^* is smeared out with increasing H . ρ' below 100 K is less affected by the magnetic field. The features at T_c and T^* become prominent for $f = 5 \text{ MHz}$. Figs. 2(d)–2(f) show the reactive component (ρ'') for the same frequencies. Unlike the resistive component, $\rho''(T, H = 0)$ for $f = 200 \text{ kHz}$ shows an abrupt increase accompanied by a peak just below T_c . Below 200 K , $\rho''(T, H = 0)$ increases gradually but shows a clear kink at $T^* \sim 160 \text{ K}$. The features at T_c and T^* become clearly

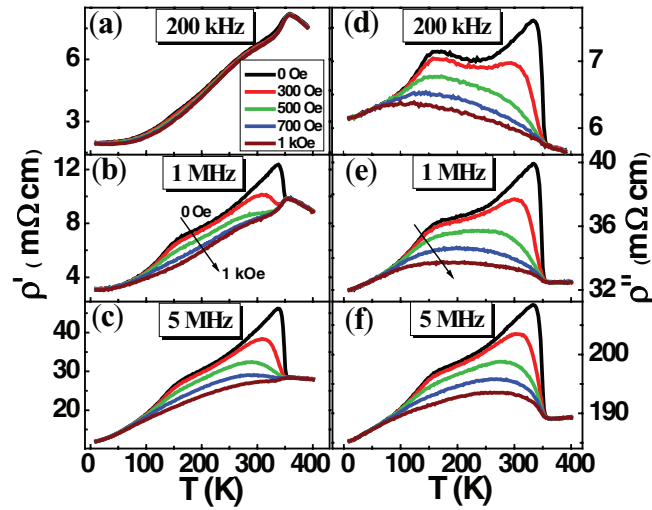


FIG. 2. Left column: Temperature dependence of the ac resistivity (ρ') under different dc magnetic fields ($H = 0, 300, 500$ Oe and 1 kOe) for (a) $f = 200$ kHz, (b) 1 MHz, and (c) 5 MHz. The right column shows the out of phase component of the resistivity (ρ'') for the same frequencies.

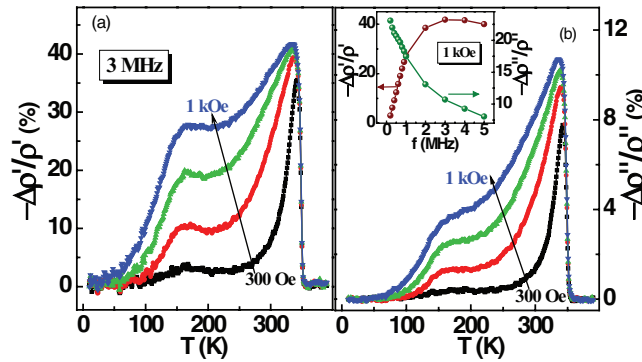


FIG. 3. Temperature dependence of (a) $(\Delta\rho'/\rho')$ and (b) $\Delta\rho''/\rho''$ at $f = 3$ MHz for different magnetic fields ($H = 300, 500, 700$ Oe and 1 kOe). The inset of (b) shows the frequency dependence of the maximum values of $\Delta\rho'/\rho'$ and $\Delta\rho''/\rho''$ at the T_c for $H = 1$ kOe.

visible at $f = 1$ and 5 MHz. As H increases in magnitude, the peak at T_c decreases in amplitude and progressively shifts towards lower temperature as like the $\rho'(T)$ at different frequencies.

We plot the temperature dependence of ac magnetoresistance ($\Delta\rho'/\rho' = [\rho'(H) - \rho'(0)]/\rho'(0)$) under different magnetic fields in Fig. 3(a) and magnetoreactance ($\Delta\rho''/\rho'' = [\rho''(H) - \rho''(0)]/\rho''(0)$) in Fig. 3(b) for $f = 3$ MHz. The ac magnetoresistance (ac MR) for $H = 300$ Oe is negligible above T_c but it increases sharply just below T_c and goes through a peak value ($= 35\%$), decreases sharply below the T_c and then changes slowly as T decreases. A weak anomaly in ac MR occurs around 147 K and the MR becomes negligible below 50 K. The magnitude of the ac MR peak at T_c increases as H increases ($= 42\%$ for $H = 1$ kOe) and so does the anomaly around 147 K. Features similar to the ac MR are seen in the magnetoreactance (MX) as well. The magnitude of MX at the peak increases from 7.8% for $H = 300$ Oe to 10.8% for $H = 1$ kOe. We show frequency dependence of the peak values of ac MR and MX for $H = 1$ kOe in the inset of Fig. 3(b). The ac MR is negligible below 1 kHz, increases with increasing f and reaches a maximum value ($= 40\text{--}45\%$) in the frequency range $f = 2\text{--}3$ MHz and then decreases slightly at higher frequencies. On the other hand, MX has the highest value of 42% at 100 kHz and it decreases monotonically with increasing frequency.

Now let us look at the field dependences of magnetoresistance and magnetoreactance. Fig. 4(a) shows the magnitude of ac MR ($\Delta\rho'/\rho'$) as a function of magnetic field at room temperature for

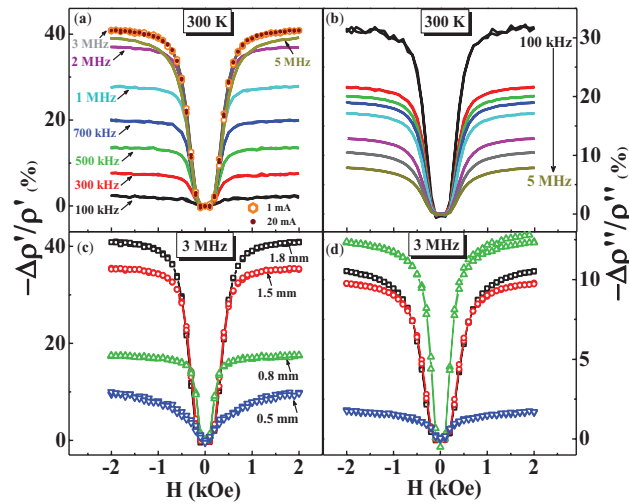


FIG. 4. (a) Field dependence of ac magnetoresistivity $\Delta\rho'/\rho'$ at different frequencies at 300 K for $I = 5$ mA. The data for $I = 1$ mA and 20 mA are identical as shown for $f = 3$ MHz. (b) Field dependence of $\Delta\rho''/\rho''$. (c) and (d) are field dependence of $\Delta\rho'/\rho'$ and $\Delta\rho''/\rho''$ at 3 MHz for different sample thicknesses ($2t$) at room temperature.

different frequencies. The ac MR is less than 2% when $f = 100$ kHz but at higher frequencies it shows a rapid increase in the field range $-500 \text{ Oe} \leq H \leq 500 \text{ Oe}$ and slow variations for H above ± 1 kOe. The magnitude of ac MR increases with f and reaches a maximum value of 41% at $f = 3$ MHz and then decreases to 39% at 5 MHz. On the other hand, the magnitude of $\Delta\rho''/\rho''$ as shown in Fig. 4(b) decreases continuously with increasing frequency. The magnitudes of ac MR and MX for $I = 1$ mA and 20 mA are same at 3 MHz, which suggests that the induced voltage is linearly proportional to the current.

We have also investigated the influence of thickness on the observed ac MR and ac MX . While the current and voltage contacts were kept intact, the bottom surface of the sample was thinned down with a fine emery paper and the field dependence of the impedance was measured for three different thicknesses at room temperature. Figs. 4(c) and 4(d) show the influence of the thickness of the sample on the ac MR and ac MX , respectively. The magnitude of the ac MR decreases dramatically with decreasing thickness of the sample whereas the ac MX initially increases with decreasing thickness and then decreases. However, the resistivity of the sample remains unaffected by the change in thickness. In Fig. 5 we show the thickness dependence of the maximum ac MR and ac MX at $H = 1$ kOe explicitly as a function of frequency. It is clear from Fig. 5(a) that with decreasing thickness of the sample, the frequency, at which the maximum ac MR occurs, shifts to higher frequency and also the maximum decreases in magnitude. For 0.5 mm thickness, the maximum shifts above 5 MHz. The ac MX also shows thickness dependence which seems to be more enhanced as the thickness reduces below 0.8 mm.

The observed features in R and X in the absence of an external dc magnetic field closely mirrors the features found in the ac inductance (ac susceptibility) or the low field (100 Oe) dc magnetization. Before seeking explanation of how the ac transport bears the imprints of magnetization, let us briefly discuss the origin of the low temperature maximum in $M(T)$ at T^* within the long range ordered ferromagnetic state. The low temperature magnetic anomaly is neither due to spin glass transition nor due to increase in the coercivity since $M(T)$ decreases even for $H = 5$ kOe although the coercivity is only 215 Oe even at 10 K. As mentioned in the introduction, recent results indicate ordering of $\text{Sm}^{3+}(4f)$ induced by the molecular field of the canted antiferromagnetic Mn sublattice in SmMnO_3 . Upon hole doping, $\text{Sm}_{1-x}\text{Sr}_x\text{MnO}_3$ becomes ferromagnetic for $0.3 \leq x \leq 0.5$ and La substitution at the Sm site as in $\text{Sm}_{0.7-x}\text{La}_x\text{Sr}_{0.3}\text{MnO}_3$ increases the Mn-O-Mn bond angle, which increases the e_g electron band width and eventually the T_c . The increased molecular field felt by the Sm site can cause the 4f moments of Sm to order at higher temperature. However, the concentration of Sm decreases with increasing La content. Hence, the occurrence of the anomaly at temperature as high as $T^* = 147$ K

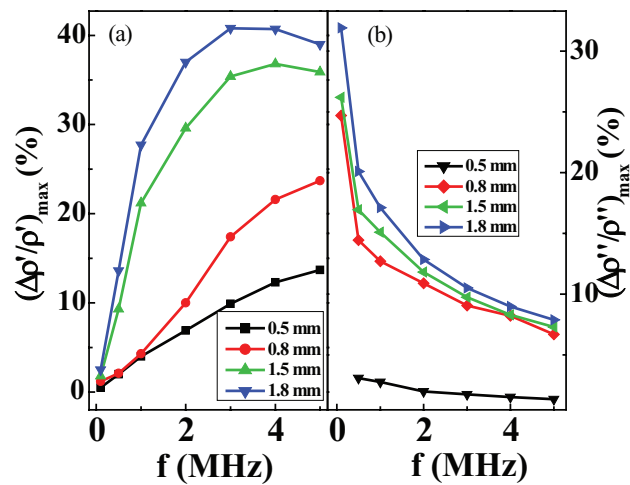


FIG. 5. Frequency dependence of the maximum values of (a) $\Delta\rho'/\rho'$ and (b) $\Delta\rho''/\rho''$ at T_c for different sample thicknesses

in $\text{Sm}_{0.1}\text{La}_{0.6}\text{Sr}_{0.3}\text{MnO}_3$ is difficult to be attributed to ordering of Sm-moment alone. We believe that there occurs a spin reorientation transition in the Mn sublattice that is driven by competition between single ion anisotropy of Sm^{3+} ions, magnetocrystalline anisotropy Mn sublattice and Sm-Mn ferrimagnetic interaction. As the external magnetic field increases above a certain value, the 4f moment tends to rotate towards the external magnetic field which weakens the 4f-3d ferrimagnetic interaction and the SRT temperature shifts to lower temperature which explains the shift of the maximum in field cooled $M(T)$ shown in Fig. 1(b). While detailed studies of magnetization in single crystalline $\text{Sm}_{0.7}\text{Sr}_{0.3}\text{MnO}_3$ are not available, magnetization in single crystalline $\text{Sm}_{0.55}\text{Sr}_{0.45}\text{MnO}_3$ shows anisotropic behavior below $T^* = 40$ K well below the onset of ferromagnetic transition ($T_c \approx 125$ K).¹² Magnetization value along $\langle 111 \rangle$ axis is higher at 60 K than at 10 K, which indicates that the ferromagnetic moment turns away from the $\langle 111 \rangle$ axis with decreasing temperature i.e., a spin reorientation transition (SRT) occurs around T^* . F. Tsui *et al.*¹⁴ reported a SRT in $\text{La}_{0.7}\text{Sr}_{0.3}\text{MnO}_3$ thin films grown on different substrates. The SRT in LSMO thin films was suggested to competition between the relative strength of the uniaxial and biaxial anisotropies. However, we did not see evidence for SRT in our bulk $\text{La}_{0.7}\text{Sr}_{0.3}\text{MnO}_3$ sample. The origin of SRT in our bulk samples of Sm-doped $\text{La}_{0.7}\text{Sr}_{0.3}\text{MnO}_3$ is different from the mechanism proposed for LSMO thin films. Although SRT has been frequently reported in canted antiferromagnets such as orthochromites, orthoferrites and in few manganites (RMO_3 , $\text{R} = \text{Pr, Gd, Ho, Sm}$ etc, $\text{M} = \text{Cr, Fe, Mn}$),¹⁷ it is seldom reported in bulk ferromagnetic manganites. Yu *et al.*¹⁸ reported a rotation of the easy axis magnetization away from c-axis with decreasing temperature in $x = 0.05$ and 0.07 single crystalline samples of $\text{La}_{1.8}\text{Sr}_{1.2}(\text{Mn}_{1-y}\text{Ru}_y)\text{O}_7$ series and attributed it to the competition between uniaxial anisotropy of Ru spins and antiferromagnetic interaction between the Ru and Mn spins.

Now let us focus on the origin of the anomalies in the ac electrical transport. The occurrence of a large ac MR ($\approx 35\%$) in a low magnetic field of $H = 300$ Oe at T_c is remarkable since the dc magnetoresistance is only 27% at T_c even at $H = 50$ kOe. The low field ac MR , unlike the high field dc MR , approaches zero at the lowest temperature. Low-field dc magnetoresistance in polycrystalline manganites is generally attributed to the enhanced tunneling of spin polarized electrons between ferromagnetic grains as their magnetizations reorient towards the direction of the applied magnetic field.¹⁹ However, the temperature and thickness dependences of ac magnetoresistance indicate that its origin is most likely macroscopic in nature in the metallic sample studied here.

Theoretical models to explain ac magnetotransport in manganites are currently not available. One possible scenario is that the e_g electrons hop shorter distance with increasing frequency of the ac current and the critical scattering by the magnetic moments of localized t_{2g} spins causes a rapid increase of the ac resistivity at T_c . However, such a critical scattering cannot explain why the magnetoresistance is dependent on the thickness of the sample. An alternative scenario is to consider

the ac electrical response of the sample as a combination of contributions arising from the resistive and reactive behaviors. We assume that ac impedance of our sample i.e., $Z(f, T, H) = R(f, T, H) + iX(f, T, H)$ can be modeled as a series combination of a resistance (R) and an inductor with reactance $X = 2\pi fL$ where L is self inductance. Hence, $\rho' \propto R$ and $\rho'' \propto X$. The flow of ac current in the sample creates a transverse ac magnetic field perpendicular to the direction of current flow. For a current of 5 mA rms, the ac magnetic field ($H_{ac} = \mu_0 I / 2\pi r$) on the surface of the sample is 0.1 mOe if we assume the sample as a cylinder with radius equal to half thickness. The ac magnetic field thus created interacts with the magnetization of the sample. At low frequencies, skin effect is negligible and the ac current flows through the bulk of the sample. As the frequency increases, current tends to migrate towards surface of the sample and becomes confined to a skin depth layer of thickness, $\delta = \sqrt{(\rho_{dc} / \pi f \mu_0 \mu_t)}$ that depends not only on the frequency (f) of the ac current and dc resistivity (ρ_{dc}) of the sample but also on the transverse magnetic permeability (μ_t) of the sample. Magnetic field can affect the skin depth via transverse permeability and a large magnetoimpedance effect was initially reported in amorphous and nanocrystalline ferromagnetic ribbons.²⁰

The ac impedance of a conducting slab of thickness $2t$ is given by

$$Z = R_{dc} k t \coth(kt) \quad (1)$$

where $k = (1+i)/\delta$ is the wave propagation constant.^{8,19}

In the low frequency limit, $\delta > t$ or $kt < 1$, Z can be approximated as,

$$Z \approx R_{dc} [1 + (kt)^2/3] = R_{dc} [1 + i \frac{2t^2 \pi f^2 \mu_0 \mu_t}{3\rho_{dc}}] \quad (2)$$

Substituting $\mu_t = \mu_t' - i\mu_t''$ and rewriting in the form $Z = R + iX$, we get

$$R = R_{dc} \left[1 + \frac{2t^2 \pi f \mu_0 \mu_t''}{3\rho_{dc}} \right], \quad X = R_{dc} \left[\frac{2t^2 \pi f \mu_0 \mu_t'}{3\rho_{dc}} \right] \quad (3)$$

Thus, the inductive reactance is proportional to $f\mu_t'$ and the excess resistance (excess to the dc resistance) is proportional to $f\mu_t''$. As the sample enters the ferromagnetic state from high temperature, μ_t' increases rapidly at $T = T_c$. Hence, the $X(T)$ or the $\rho''(T)$ increases rapidly at T_c even in the absence of an external magnetic field. Below the SRT, μ_t' decreases and it is reflected in the decrease of $\rho''(T)$ below 160 K. The μ_t'' which characterizes the magnetic loss is small at $f = 200$ kHz and hence the $\rho'(T)$ is not affected at this frequency. However, as the frequency increases, μ_t' is expected to decrease rapidly above a characteristic frequency and μ_t'' is expected to go through a maximum value due to domain relaxation process. In the ferromagnetic state, the ac permeability of polycrystalline $\text{La}_{0.7}\text{Sr}_{0.3}\text{MnO}_3$ shows relaxation behavior: μ_t' starts to decrease rapidly ~ 1 MHz around which μ_t'' goes through a maximum value due to relaxation of domain walls.²¹

As the frequency increases, the ac current tends to migrate towards the surface due to skin effect. If the skin depth is much smaller than the half thickness of the sample ($\delta \ll t$), then the impedance takes the form²⁰

$$Z = R_{dc}(1 + i)\rho_{dc}/\delta = R_{dc}(a/2\delta_0)(\sqrt{\mu_R} - i\sqrt{\mu_L}) \quad (4)$$

where $\mu_R = |\mu_t| + \mu_t''$, $\mu_L = |\mu_t| - \mu_t''$ and δ_0 is the non magnetic skin depth. Thus, if we take $Z = R + iX$, then $R = (\omega\rho)^{1/2} \sqrt{|\mu_t| + \mu_t''}$ and $X = (\omega\rho)^{1/2} \sqrt{|\mu_t| - \mu_t''}$. Thus, in the high frequency skin depth dominated regime, both resistance and reactance are affected by the magnetic loss (μ_t'').

The nonmagnetic skin depth in the paramagnetic state of our sample, for instance at $T = 348$ K ($> T_c$) is 6 mm which is larger than the half thickness of the sample ($t = 0.9$ mm). As the sample enters the ferromagnetic state from paramagnetic state, the skin depth is expected to decrease in zero external magnetic field because the transverse ac magnetic permeability (μ_t) increases abruptly at $T = T_c$. If we take $\mu_t = 50$ in our sample (somewhat smaller than $\mu = 85$ in $\text{La}_{0.7}\text{Sr}_{0.3}\text{MnO}_3$),²¹ the magnetic skin depth at $T = T_c$ becomes 0.65 mm for $f = 1$ MHz, which is smaller than half thickness of the sample ($t = 0.9$ mm). As the cross sectional area for the current flow decreases at T_c , both the components of the resistivity show abrupt increase, followed by decrease at T^* due to decrease in μ_t below T^* . In the presence of a dc magnetic field, the dc magnetization of magnetic

domains predominantly align along the field direction and the magnetic response of domains to small ac magnetic field becomes weaker, i.e., ac permeability decreases. As a result, the skin depth increases at T_c and hence the ac resistivity decreases with increasing magnetic field. The observed thickness dependence of the ac magnetoresistance supports the scenario that we are dealing with skin depth related phenomena. In thicker sample, $\delta \ll t$ and for thin sample, $\delta > t$, where t is the half thickness. The skin effect is less important in thinner sample. With increasing frequency, the skin depth is expected to decrease provided that the transverse permeability is frequency independent. However, we notice that magnetoresistance in thick sample reaches a maximum value for $f = 2\text{--}3$ MHz. This frequency corresponds to the characteristic relaxation frequency of domain rotation (i.e. where μ_t'' exhibits a maximum value). Since μ'' starts decreasing above this frequency, the applied magnetic field has less impact on its value and hence the ac magnetoresistance also decreases.

IV. SUMMARY

In summary, we have investigated magnetic, dc and ac electrical transport properties in $\text{Sm}_{0.1}\text{La}_{0.6}\text{Sr}_{0.3}\text{MnO}_3$. It is found that with increasing frequency of the ac current, anomalies develop in the ac resistance and the reactance at the Curie temperature and at a temperature T^* much below T_c in zero magnetic field. The magnetic anomaly at $T^* \ll T_c$ is suggested to be caused by spin reorientation transition of the Mn-sublattice promoted by ferrimagnetic 4f-3d interaction. The observed anomalies are suppressed in sub-kilogauss dc magnetic fields leading to a huge ac magnetoresistance ($= 35\%$ in $\Delta H = 300$ Oe). It is suggested that high frequency magnetotransport is dominated by the temperature, field and frequency dependence of the ac permeability. Thus, magnetic control of the ac permeability provides an alternative method to enhance the value of low-field magnetoresistance in manganites. To gain better understanding of the ac magnetotransport, it will be worthy to investigate magnetoimpedance of epitaxial thin films with varying thickness.

ACKNOWLEDGMENTS

R. M. acknowledges the Ministry of Education, Singapore (Grant. No R144-000-308-112) for supporting this work.

- ¹ J. M. D Coey, M. Viret, and S. von Molnar, *Adv. Phys.* **58**, 571 (2009).
- ² C. Zener, *Physical Review* **82**, 403 (1951).
- ³ W. Prellier, M. P. Singh, and P. Murugavel, *J. Phys. Cond. Mater.* **17**, R803 (2005).
- ⁴ T. Goto, T. Kimura, G. Lawes, A. P. Ramirez, and Y. Tokura, *Phys. Rev. Lett.* **92**, 257201 (2004).
- ⁵ R. Schmidt, J. Ventura, E. Langenberg, N. M. Nemes, C. Munuera, M. Varela, M. García-Hernández, C. León, and J. Santamaría, *Phys. Rev. B* **86**, 035113 (2012).
- ⁶ E. Langenberg, I. Fina, J. Ventura, B. Noheda, M. Varela, and J. Fontcuberta, *Phys. Rev. B* **86**, 085108 (2012).
- ⁷ S. M. Bhagat, S. E. Lofland, P. H. Kim, D. C. Schmadel, C. Kwon, R. Ramesh, and S. D. Tyagi, *J. Appl. Phys.* **81**, 5157 (1997).
- ⁸ A. Schwartz, M. Scheffler, and S. M. Anlage, *Phys. Rev. B* **61**, R870 (2000).
- ⁹ H. Qin, J. Hu, B. Li, Y. Hao, J. Chen, and M. Jiang, *J. Magn. Magn. Mater.* **320**, 2770 (2008).
- ¹⁰ A. Rebello and R. Mahendiran, *Euro. Phys. Lett.* **86**, 27004 (2009); *Appl. Phys. Lett.* **96**, 032502 (2010).
- ¹¹ V. B. Naik and R. Mahendiran, *J. Appl. Phys. Lett.* **110**, 053915 (2011).
- ¹² V. Y. Ivanov, A. A. Mukhin, A. S. Prokhorov, and A. A. Balbashov, *Phys. Stat. Sol. B* **236**, 445 (2003).
- ¹³ J. G. Cheng, J. S. Zhou, J. B. Goodenough, Y. T. Su, Y. Sui, and Y. Ren, *Phys. Rev. B* **84**, 104415 (2011).
- ¹⁴ F. Tsui, M. C. Smoak, T. K. Nath, and C. B. Eom, *Appl. Phys. Lett.* **76**, 2421 (2000).
- ¹⁵ K. Yoshii, *J. Solid State Chem.* **159**, 204 (2000); *Appl. Phys. Lett.* **99**, 142501 (2011).
- ¹⁶ J.-H. Lee, J. K. Jeong, J. H. Park, M. A. Oak, H. M. Jang, J. Y. Son, and J. F. Scott, *Phys. Rev. Lett.* **107**, 117201 (2012).
- ¹⁷ F. Hong, Z. Cheng, and Z. Wang, *Appl. Phys. Lett.* **99**, 192503 (2011).
- ¹⁸ X. Z. Yu, M. Uchida, Y. Onose, J. P. He, Y. Kaneko, T. Asaka, K. Kimoto, Y. Matsui, T. Arima, and Y. Tokura, *J. Magn. Magn. Mater.* **302**, 391 (2002).
- ¹⁹ H. Y. Hwang, S.-W. Cheong, N. P. Ong, and B. Batlogg, *Phys. Rev. Lett.* **77**, 2041 (1996).
- ²⁰ L. V. Panina, K. Mori, T. Uchiyama, and M. Noda, *IEEE Trans. Magnetics*, **31**, 1249 (1995).
- ²¹ J. Wang, G. Liu, G. Nie, and Y. Du, *J. Magn. Magn. Mater.* **280**, 316 (2004).